BIOCHEMISTRY
including biophysical chemistry & molecular biology

ARTICLE

pubs.acs.org/biochemistry

# Binding Stoichiometry and Affinity of the Manganese-Stabilizing Protein Affects Redox Reactions on the Oxidizing Side of Photosystem II

Johnna L. Roose,[§] Charles F. Yocum,[†,‡] and Hana Popelkova*[,†]

[†]Department of Molecular, Cellular and Developmental Biology and [‡]Department of Chemistry, The University of Michigan, Ann Arbor, Michigan 48109-1048, United States

[§]Department of Biological Sciences, Division of Biochemistry and Molecular Biology, Louisiana State University, Baton Rouge, Louisiana 70803, United States

Supporting Information

**ABSTRACT:** It has been reported previously that the two subunits of PsbO, the photosystem II (PSII) manganese stabilizing protein, have unique functions in relation to the Mn, $Ca^{2+}$, and $Cl^-$ cofactors in eukaryotic PSII [Popelkova; et al. (2008) *Biochemistry 47*, 12593]. The experiments reported here utilize a set of N-terminal truncation mutants of PsbO, which exhibit altered subunit binding to PSII, to further characterize its role in establishing efficient $O_2$ evolution activity. The effects of PsbO binding stoichiometry, affinity, and specificity on $Q_A^-$ reoxidation kinetics after a single turnover flash, S-state transitions, and $O_2$ release time have been examined. The data presented here show that weak rebinding of a single PsbO subunit to PsbO-depleted PSII repairs many of the defects in PSII resulting from the removal of the protein, but many of these are not sustainable, as indicated by low steady-state activities of the reconstituted samples [Popelkova; et al. (2003) *Biochemistry 42*, 6193]. High affinity binding of PsbO to PSII is required to produce more stable and efficient cycling of the water oxidation reaction. Reconstitution of the second PsbO subunit is needed to further optimize redox reactions on the PSII oxidizing side. Native PsbO and recombinant wild-type PsbO from spinach facilitate PSII redox reactions in a very similar manner, and nonspecific binding of PsbO to PSII has no significance in these reactions.

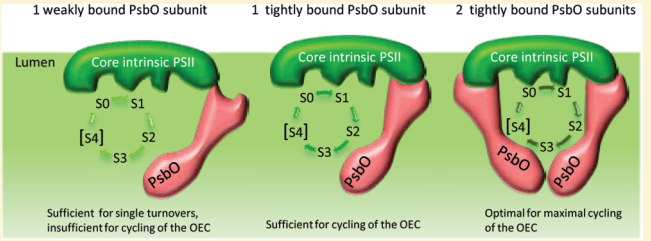


Oxygenic photosynthetic organisms employ the redox enzyme called photosystem II (PSII) that includes a module called the oxygen-evolving complex (OEC) containing an active site comprised of 4Mn, $1Ca^{2+}$, and $1Cl^-$. The Mn and $Ca^{2+}$ cofactors are bound by amino acid side chains of the intrinsic chlorophyll-binding polypeptides D1 and CP43, which along with D2, CP47, and the α and $\beta$ subunits of cytochrome $b_{559}$ make up the core PSII reaction center.[1,2] The OEC active site is coordinated on the lumenal side of thylakoid membranes and is shielded from endogenous reducing agents (such as quinones) by a set of at least three extrinsic proteins. The OEC catalyzes light-driven water oxidation, where two molecules of $H_2O$ are oxidized to $O_2$, $4H^+$, and four electrons.[3,4] Upon illumination, the OEC cycles through five distinct redox states, called the S-states ($S_n$, where $n = 0-4$ and $S_1$ is the dark-stable state).[1,5] The electrons are transferred from the OEC through other cofactors associated with PSII, including a redox-active tyrosine (Yz) and two separate plastoquinones ($Q_A$ and $Q_B$). From PSII, electrons are further shuttled via reduced plastoquinone to other multisubunit membrane protein complexes of the photosynthetic electron transfer chain.[1,3]

In addition to shielding the OEC from exogenous reductants, the PSII extrinsic proteins also function to increase the efficiency of PSII redox reactions.[6−11] Composition of these proteins varies widely among different photosynthetic organisms, but it is generally accepted that PSII from higher plants and green algae contains the PsbO, PsbP, and PsbQ subunits, while cyanobacterial and red algal PSII bind PsbO, PsbV, and PsbU polypeptides and also possess analogues of PsbP and PsbQ.[12] In higher plants and green algae, the smaller extrinsic proteins PsbP and PsbQ regulate retention of $Ca^{2+}$ and $Cl^-$ by PSII.[13,14] The PsbP polypeptide is also required to maintain the active Mn cluster *in vivo* as well as for PSII core assembly and stability.[11,15] PsbQ was also found to be an important component for assembly and stability of PSII and to be essential for photoautotrophic growth under low light conditions.[16] In cyanobacterial PSII, PsbV has been proposed to play a stabilizing role in PSII and to retain $Ca^{2+}$ and $Cl^-$ in the OEC. The PsbU protein has been suggested to stabilize the OEC against oxidative and heat stresses and to function to minimize the $Ca^{2+}$ and $Cl^-$ requirements for $O_2$ evolution.[10]

The largest extrinsic subunit, PsbO, is required for stabilization of the Mn cluster and for facilitation of high rates of $O_2$

**Received:** January 25, 2011
**Revised:** June 10, 2011
**Published:** June 10, 2011

**Table 1. PsbO Binding Affinities and $O_2$ Evolution Activities of Intact PSII, SW-PSII, UW-PSII Membranes, and PsbO-Depleted PSII Reconstituted with Recombinant Wild-Type or Mutated PsbO's**

| | | binding (mol PsbO/mol PSII) | |
|---|---|---|---|
| sample | activity[a] (% of control) | specific | nonspecific |
| intact PSII | 170 | 2 | 0 |
| SW-PSII | 100 | 2 | 0 |
| UW-PSII[b] | 0 | 0 | 0 |
| UW-PSII + WT PsbO | 70 | 2 | 0 |
| UW-PSII + ΔG3M | 80 | 2 | ∼4 |
| UW-PSII + ΔK14M | 50 | 1 | ∼3 |
| UW-PSII + ΔT15M | 20 | 0.5 | ∼0.5 |

[a] The actual rates of $O_2$ evolution activity of control samples were as follows: 550−650 μmol $O_2$/mg Chl/h for intact PSII, 250−350 μmol $O_2$/mg Chl/h for SW-PSII, and 90−150 μmol $O_2$/mgChl/h for UW-PSII. [b] Residual activity of UW-PSII was subtracted from that of all samples before percent activities were calculated. Data from refs 36, 39, and 40.

evolution. Some PsbO acidic residues deprotonate during the $S_1 \rightarrow S_2$ transition of the OEC, the protein structure undergoes changes upon reduction of the Mn cluster,[17,18] and PsbO also facilitates $Cl^-$ retention by PSII.[19−21] That PsbO is indispensible for optimal PSII function and structural stability is evidenced by numerous studies documenting the consequences of the absence of the PsbO protein. Biochemical extraction of PsbO from spinach PSII was shown to retard recombination of $Q_A^-$ with the PSII oxidizing side, to increase the probability for aberrant S-state transitions (especially double hits), to change the S-state distribution, to increase the dark stability of the $S_2$ and $S_3$ states, to retard the transition from $S_3$ to the $S_0$ state, and to delay $O_2$ release after the third flash.[22−24] Very similar results on the dark stability of the higher S-states and $O_2$-release kinetics were observed in the Δ*psbO* strain from the cyanobacterium *Synechocystis sp.* PCC 6803, but an increased miss factor and retardation of reduction of photooxidized $Y_z^\bullet$ were also reported.[25,26] An *Arabidopsis* mutant that is defective in the *psb*O-1 gene, but not in a second (*psb*O-2) gene, exhibited growth retardation,[27] longer $S_2$ and $S_3$ lifetimes, elevated levels of $PSII_\beta$ reaction centers, slower electron transfer from $Q_A^-$ to $Q_B$,[28,29] and a defect in $Ca^{2+}$ retention.[29] Suppressed expression of both *Arabidopsis psb*O genes by RNAi resulted in the loss of variable fluorescence, stabilization of the $S_2$ state, significant loss of the CP47, CP43, D1, and PsbQ polypeptides from PSII, and the loss of photoautrophy.[30] Loss of PSII core proteins and an inability to grow photoautotrophically were also observed in the PsbO-less mutant from *Chlamydomonas reinhardtii*.[31]

A number of experimental studies suggest that two PsbO subunits are bound per eukaryotic PSII reaction center.[32−38] A previous study, which determined the effect of PsbO stoichiometry on the Mn, $Ca^{2+}$, and $Cl^-$ cofactors in PSII, has shown that a single PsbO subunit is sufficient to stabilize the Mn cluster and enhance $Cl^-$ retention by the OEC, while two PsbO subunits are needed for efficient $Cl^-$ retention, which correlates with maximal $O_2$ evolution activity.[20]

This work examines the effects of PsbO binding stoichiometry, affinity, and specificity on PSII electron transfer and turnover of the OEC. PSII membranes reconstituted with different PsbO mutants with defined PSII binding properties (see Table 1) are characterized here using fluorescence decay and flash oxygen yield experiments. The data show that PsbO stoichiometry and binding affinity in PSII have complex, wide-ranging effects on the redox properties of the oxidizing side of PSII and that any nonspecific binding of PsbO to PSII by any of the recombinant proteins has no impact on PSII function.

## MATERIALS AND METHODS

**PSII Preparations.** Several spinach PSII preparations with different PsbO binding characteristics were used to determine the effect of PsbO binding affinity and stoichiometry on PSII function. These are UW-PSII reconstituted with various mutated PsbO proteins that exhibit different binding stoichiometries and affinities and three control samples: UW-PSII (PsbO-depleted PSII prepared by treating NaCl-washed PSII with ∼2.6 M urea and 0.2 M NaCl), SW-PSII (NaCl-washed PSII membranes depleted of PsbP and PsbQ extrinsic proteins that retain two natively assembled PsbO subunits), and intact PSII (which contains a complete set of natively bound extrinsic proteins; two subunits of PsbO, one each of PsbP and PsbQ). Oxygen evolution activities and PsbO binding properties of samples used in this study are summarized in Table 1. Details of other characteristics of these PsbO deletion mutants are given in refs 36, 39, and 40.

**Reconstitution of PsbO-Depleted PSII with Recombinant PsbO.** The intact PSII, SW-PSII, and UW-PSII membranes were prepared and stored as described in ref 39. The UW-PSII membranes were reconstituted with recombinant PsbO proteins (5 mol PsbO/mol PSII to ensure maximum binding) for 1 h at room temperature in a reconstitution buffer containing 37 mM MES (pH 6), 100 μg/mL BSA, 0.3 M sucrose, 2% betaine (w/v), and saturating concentrations of $Ca^{2+}$ (10 mM) and $Cl^-$ (110 mM). The Chl concentration in the reconstitution mixtures was 200 μg/mL. The 1 mL aliquots of the reconstitution mixtures were centrifuged at 10 000*g* and 4 °C for 10 min. Each pellet was resuspended in 65 μL of reconstitution buffer to obtain samples with Chl concentrations of 3 mg/mL. Aliquots (15 μL) of resuspended samples were stored at −70 °C.

**Fluorescence Experiments.** Fluorescence decay after a single saturating flash was monitored with a Photon Systems Instruments (PSI) FL3000 dual modulation kinetic fluorimeter (a commercial version of the instrument described in ref 41). Both measuring and saturating flashes were provided by computer-controlled photodiode arrays. All samples were dark adapted for 5 min prior to measurement. Samples were assayed for fluorescence decay in reconstitution buffer at 10 μg chlorophyll/mL. Similar results were also obtained with identical samples in assay buffer (0.4 M sucrose, 50 mM MES-NaOH, pH 6.0, 10 mM $CaCl_2$, 80 mM NaCl). The fluorescence decay experiments monitored forward electron transfer from $Q_A^-$ to $Q_B$ in the absence of DCMU and charge recombination between $Q_A^-$ and the PSII oxidizing side in the presence of DCMU (10 μM). The experimental data were analyzed using mathematical fitting that included three exponential decay components and one long-lived residual ($\tau > 10$ s) component.[42] Data analysis was carried out using the Origin (version 6.1) program and software provided by Photon Systems Instruments. For each fluorescence trace, $F_M$ was normalized on the fluorescence value measured at the time of the flash.

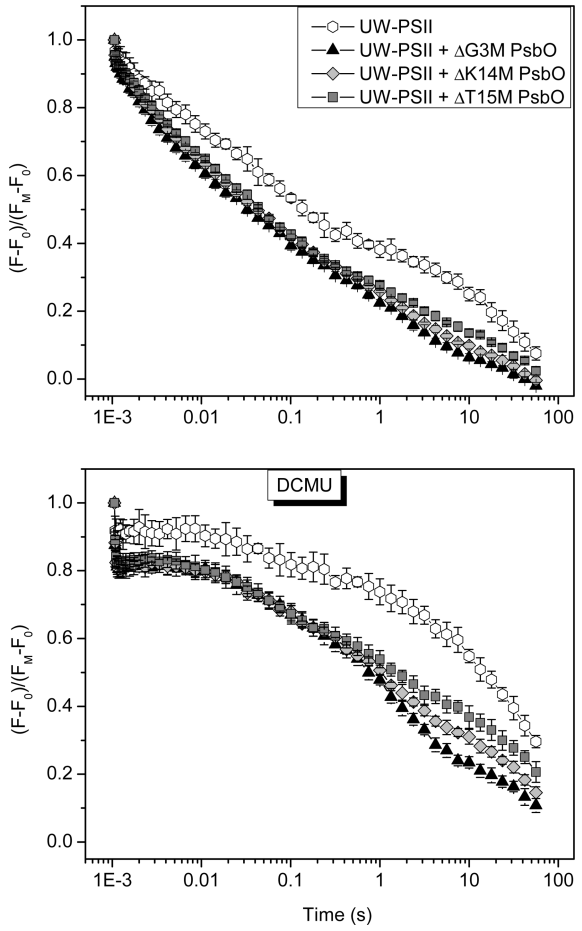


**Figure 1.** $Q_A^-$ reoxidation kinetics in the absence (upper panel) or presence (lower panel) of 10 $\mu$M DCMU after a single saturating flash applied to UW-PSII reconstituted with ΔG3M PsbO, ΔK14M PsbO, or ΔT15M PsbO. Data for PsbO-depleted sample, which is shown in each panel as the control for purposes of comparison, are taken from ref 23. Data were collected after dark incubation for 5 min. Points are the averages, and vertical bars at each point give the standard deviation; $n = 6-9$.

**Oxygen Flash Yield Measurements.** The flash $O_2$ yield measurements were performed on a bare platinum electrode (Artesian Scientific Co., Urbana, IL). Photosystem II membrane samples containing 2.5−10 $\mu$g of chlorophyll in the assay buffer used for the fluorescence experiments were applied to the bare platinum electrode, covered with an agarose disk (1% agarose in assay buffer), and dark incubated for 5 min; extension of the dark incubation period to 20 min resulted in low signal intensities and artifacts in the $O_2$ peaks (data not shown). The electrode was polarized at +0.73 V for 20 s, and a series of 50 saturating flashes at 0.3 s intervals were supplied by an integrated, computer-controlled xenon flash lamp. S-state distributions and parameters were calculated by fitting using a four-state homogeneous model.[43] The $O_2$ rise times were calculated by fitting peaks to the equation $f(t) = a + b(1 - e^{-krt}) + ce^{-kdt}$ using the Origin 6.1 software package. The corresponding $t_{1/2}$ values for the rise of the $O_2$ signals were calculated by $t_{1/2} = 0.693/k_r$.

## RESULTS

**Fluorescence Decay Kinetics.** In the absence of DCMU, fluorescence decay kinetics in PSII are dominated by forward electron transfer from $Q_A^-$ to $Q_B$ on the reducing side, with a small contribution from slower charge recombination with the oxidizing side.[44−48] Significant effects of removal of native extrinsic polypeptides from PSII on fluorescence decay kinetics have been characterized,[23,24] as described in the Introduction. Decay curves from UW-PSII and samples reconstituted with ΔG3M, ΔK14M, or ΔT15M PsbO are presented in Figure 1, upper panel, which exhibit increased decay rates relative to the UW-PSII control (open circles) but show relatively small differences among themselves. The kinetic parameters in Table 2 fit these decay curves to three exponential components according to ref 42: a fast component due to electron transfer between $Q_A^-$ and $Q_B$,[44,45] an intermediate component that is ascribed to the transfer of an electron from $Q_A^-$ to $Q_B$ in PSII centers where plastoquinone has to bind to the $Q_B$ site before the electron is transferred from $Q_A^-$,[46] and a slow decay component that reflects charge recombination between $Q_A^-$ and the PSII oxidizing side.[47] The residual fraction has been attributed to the equilibrium between $Q_A^-$ and $Q_B$.[48]

Rebinding of any PsbO mutant significantly increases the amplitude of the fast phase and shortens the decay kinetics of the intermediate and slow phases. At the same time, if one compares the results for each mutant, it is seen that the parameters and traces for the fast and intermediate phases of the fluorescence decay are very similar for all PsbO-reconstituted samples, indicating that stoichiometry and binding affinity of PsbO on the oxidizing side of PSII have a negligible effect on forward electron transfer from $Q_A^-$ to $Q_B$. More significant differences among truncation mutants of PsbO are observed for the slow phase, which reflects charge recombination between $Q_A^-$ and the oxidizing side of PSII. Weak rebinding of one copy of PsbO (Δ*T*15M) significantly lowers the slow decay time values relative to those observed for UW-PSII (6.2 s vs 17 s[23]), and high-affinity binding of a single copy of PsbO to PSII (ΔK14M) further decreases these values (4 s). The values observed for the slow and residual components for ΔG3M PsbO-reconstituted UW-PSII are statistically equivalent to the corresponding values obtained for the sample containing recombinant WT PsbO,[23] indicating that, with respect to charge recombination between $Q_A^-$ and the PSII oxidizing side, PSII containing two specifically bound copies of the ΔG3M PsbO mutant does not differ from PSII containing two subunits of recombinant WT PsbO. Therefore, any nonspecific PSII-binding associated with the ΔG3M PsbO mutant does not contribute to PSII function determined by this assay. The major effects of PsbO rebinding for those components of the fluorescence decay that are significantly different from the UW-PSII samples are reflected in the amplitude of the $Q_A^- \rightarrow Q_B$ reaction and the increased slow decay rate of the recombination reaction between the reducing side and the OEC.

Addition of DCMU blocks electron transfer from $Q_A^-$ to $Q_B$ so fluorescence decay in this case is a direct reflection of charge recombination between $Q_A^-$ and components on the oxidizing side of PSII. Figure 1, lower panel, shows the effects of PsbO reconstitution on the decay kinetics and the parameters shown in Table 3 fit the fluorescence decay curves.[42] Fast decay (≤3 ms) arises from the fraction of centers in which electrons are transferred from $Q_A^-$ to $Y_z^\bullet$ owing to the absence of a functional Mn cluster.[49] The intermediate phase is associated with faster charge recombination between $Q_A^-$ and either a native or altered $S_2$ state,[42] in agreement with the short (ms) lifetimes of $Y_z^\bullet$ in PSII preparations that retain intact, nonfunctional Mn clusters.[50−52] The slow component is also attributed to charge recombination between

Table 2. Kinetic Parameters of $Q_A^-$ Reoxidation in the Absence of DCMU after a Single Saturating Flash Applied to PsbO-Depleted PSII Reconstituted with ΔG3M PsbO, ΔK14M PsbO, or ΔT15M PsbO[a]

| | fast phase | | intermediate phase | | slow phase | | |
|---|---|---|---|---|---|---|---|
| sample | $t_1$ (ms) | % amplitude | $t_2$ (ms) | % amplitude | $t_3$ (s) | % amplitude | % residual ampl |
| UW-PSII[b] | 3.0 ± 1.0 | 29 ± 1.0 | 110 ± 20 | 32.0 ± 2.0 | 17 ± 2.0 | 31.0 ± 2.0 | 8.0 ± 3.0 |
| UW-PSII + ΔG3M | 2.2 ± 0.1 | 43 ± 2.0 | 66 ± 5 | 28.1 ± 0.7 | 3.2 ± 0.2 | 27.0 ± 1.0 | 2.4 ± 0.5 |
| UW-PSII + ΔK14M | 2.6 ± 0.3 | 40 ± 0.6 | 80 ± 10 | 29.6 ± 0.5 | 4.0 ± 0.5 | 26.4 ± 0.6 | 4.0 ± 0.8 |
| UW-PSII + ΔT15M | 2.9 ± 0.4 | 38 ± 0.6 | 80 ± 10 | 32.0 ± 1.0 | 6.2 ± 0.9 | 23.7 ± 0.9 | 6.5 ± 0.8 |

[a] $n$ = 6−9; error, ±1.0 standard deviation. [b] Data from ref 23 are shown for purposes of comparison.

Table 3. Kinetic Parameters of $Q_A^-$ Reoxidation after a Single Saturating Flash Applied to DCMU-Treated PsbO-Depleted PSII Reconstituted with ΔG3M PsbO, ΔK14M PsbO, or ΔT15M PsbO Proteins[a]

| | fast phase | | intermediate phase | | slow phase | | |
|---|---|---|---|---|---|---|---|
| sample | $t_1$ (ms) | % amplitude | $t_2$ (s) | % amplitude | $t_3$ (s) | % amplitude | % residual ampl |
| UW-PSII[b] | 60 ± 20 | 13 ± 2 | 3.0 ± 2.0 | 16 ± 3 | 38 ± 16 | 51 ± 6 | 21 ± 9 |
| UW-PSI + ΔG3M | 60 ± 10 | 20 ± 2 | 1.4 ± 0.2 | 44 ± 1 | 24 ± 8 | 24 ± 2 | 12 ± 2 |
| UW-PSI + ΔK14M | 40 ± 10 | 20 ± 1 | 1.1 ± 0.1 | 32 ± 2 | 24 ± 11 | 31 ± 4 | 17 ± 5 |
| UW-PSI + ΔT15M | 50 ± 10 | 21 ± 2 | 1.2 ± 0.3 | 24 ± 2 | 33 ± 12 | 34 ± 2 | 20 ± 3 |

[a] $n$ = 6−9; error, ±1.0 standard deviation. [b] Data from ref 23 are shown for purposes of comparison.

$Q_A^-$ and the $S_2$ state and perhaps the $S_3$ state,[53] whereas the residual component arises from very slow charge recombination between $Q_A^-$ and the oxidizing side of PSII.[42]

The data in Table 3 that reveal statistically significant changes in PSII electron transfer upon rebinding of PsbO's to UW-PSII are the signal amplitudes for the intermediate and slow phases of the decay (recombination of $Q_A^-$ with native or modified S-states). Intermediate phase decay kinetics are unaffected by reconstitution with PsbO's, but a significant increase in the amplitude (from 24 to 44%) of the decay is detected with increasing PsbO affinity and binding stoichiometry. Relative to UW-PSII,[23,24] reconstitution of PsbO-depleted PSII with ΔT15M PsbO decreases the amplitude associated with the slow phase (51% to 34%), indicating that even weak rebinding of a single copy of PsbO to PSII can significantly restore the reactivity of PSII oxidizing side components created by a single turnover flash. High affinity binding of one (ΔK14M) or two (ΔG3M) PsbO subunits to PSII has a minimal effect on the kinetic properties of the slow phase, as compared to the ΔT15M sample, but the slow phase amplitudes are decreased as the intermediate phase amplitudes are increased. These results are consistent with deviations in the traces of samples beyond ∼1 s in Figure 1 (lower panel) and suggest a further recovery of normal charge recombination with the oxidizing side of PSII after a single turnover flash. In this respect, the fully functional truncated mutant ΔG3M PsbO does not differ from recombinant WT PsbO (see ref 23). Taken together, data presented in Figure 1 and Tables 2 and 3 indicate that increases in PsbO stoichiometry and/or binding affinity in PSII decreases the population of PSII centers in stable $S_2$ and $S_3$ states that form in the absence of PsbO and increases the population of centers in normal higher S-states, relative to UW-PSII.

**Oxygen Flash Yield Experiments.** The fluorescence decay data indicate that PsbO binding affinity and stoichiometry affect oxidizing side reactions in PSII and may influence the lifetimes and/or populations of the higher S-states. To obtain detailed information on cycling of the OEC through the five S-states ($S_0$−$S_4$), $O_2$ yields after a series of short saturating flashes were measured to monitor the stepwise advancement of reaction centers in samples reconstituted with mutated PsbO; samples lacking PsbO (UW-PSII) or containing native PsbO (intact PSII and SW-PSII) were used as controls. Native PSII centers typically decay back to the $S_1$ state during a dark incubation period prior to the $O_2$ yield measurement, but there is also a significant population of centers in the $S_0$ state. This produces a characteristic pattern with low $O_2$ yields after the first two flashes followed by a maximum on the third flash and a diminished $O_2$ peak on the fourth flash. In PSII preparations, the period-four oscillation in $O_2$ damps quickly during the flash train as centers become asynchronous owing to acceptor-side limitations; damping of oscillations occurs after <10−15 flashes (ref 54 and see "Intact PSII" in Figure 2).

Figure 2 shows the typical $O_2$ flash yield patterns for PsbO-depleted PSII reconstituted with the ΔG3M, ΔK14M, or ΔT15M PsbO mutants and for the controls (intact PSII and SW-PSII). The pattern for UW-PSII[23] is included for comparison. Traces were normalized to the peak height after the third flash. Intact PSII membranes display a typical $O_2$ flash yield pattern with a maximum on the third flash and a strongly diminished intensity of the $O_2$ yield on the fourth flash. Extraction of PsbP and PsbQ changes the $O_2$ flash yield pattern qualitatively; the peaks on the third and fourth flashes are followed by a fifth $O_2$ peak with a high relative intensity (Figure 2) and significant $O_2$ yields on each succeeding flash. The $O_2$ flash yield pattern for UW-PSII in Figure 2 shows that PsbO extraction from PSII results in an altered $O_2$ yield pattern where the maximum occurs on the first flash; this peak has twice the intensity of the $O_2$ yield on the third flash; its origin is discussed in detail below. Reconstitution of PsbO-depleted PSII with the ΔG3M PsbO mutant results in an $O_2$ flash yield pattern that is very similar to that of SW-PSII, except that a small $O_2$ yield is observed on the first flash. Rebinding of the ΔK14M PsbO


dx.doi.org/10.1021/bi2008068 |Biochemistry 2011, 50, 5988–5998

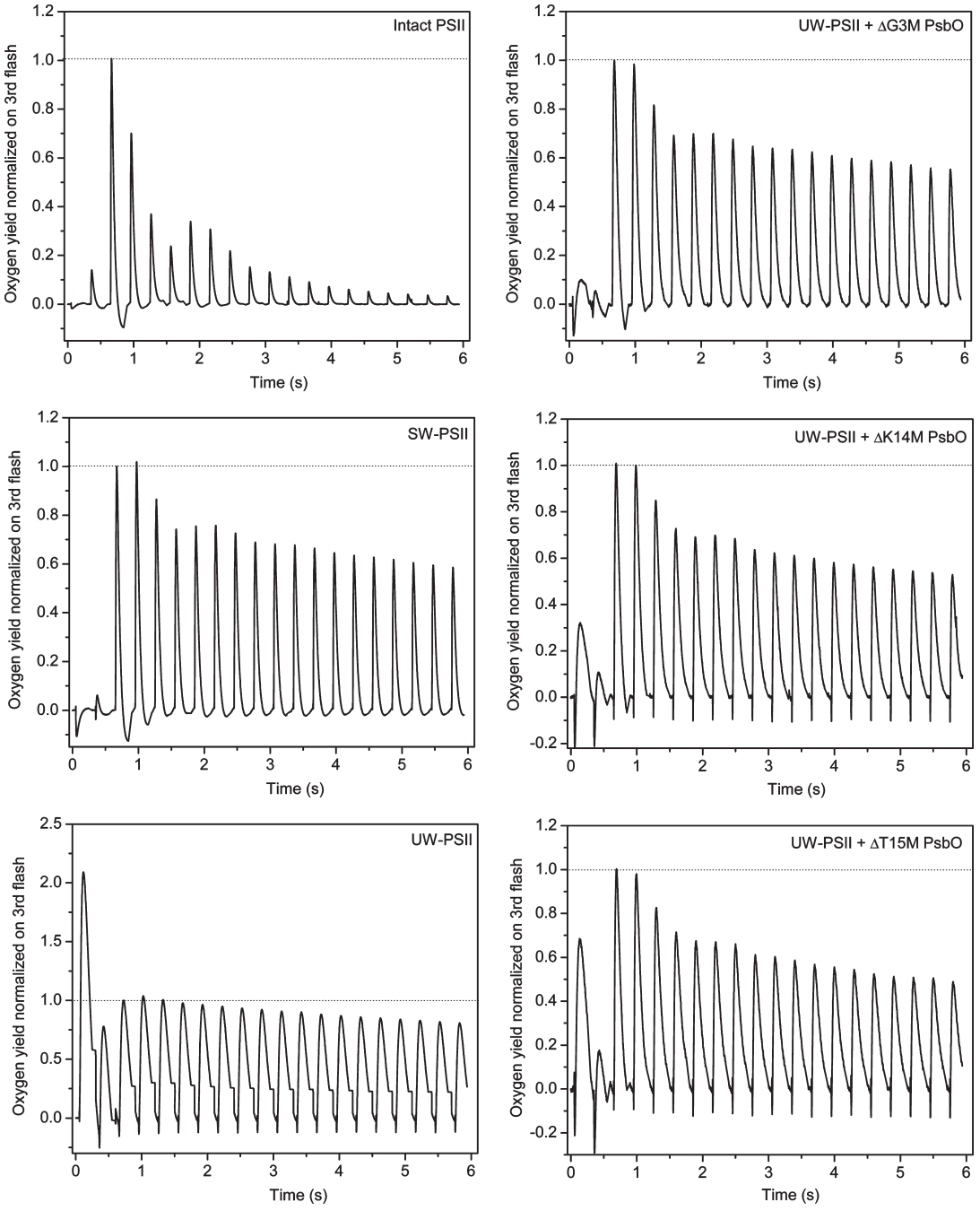


**Figure 2.** Data illustrating the typical flash $O_2$ yield patterns obtained from intact PSII, SW-PSII, and UW-PSII and from PsbO-depleted PSII reconstituted with ΔG3M PsbO, ΔK14M PsbO, or ΔT15M PsbO proteins. The pattern for UW-PSII is taken from ref 23 for comparison. Curves were normalized to the height of the third peak ($O_2$ yield after the third saturating flash).

mutant to UW-PSII produces an $O_2$ flash yield pattern similar to that detected with ΔG3M PsbO, but an $O_2$ yield on the first flash is observed with a value of ~0.3 when compared to the $O_2$ yield on the third flash. The same trend in the $O_2$ flash yield pattern is observed after reconstitution of UW-PSII with the ΔT15M PsbO mutant; in this case, the $O_2$ yield on the first flash has a relative value of ~0.7. It should be noted that $O_2$ flash yield patterns presented here originate from signals with different absolute values. The intact PSII sample exhibited a highest absolute signal with 2.5 $\mu$g of Chl per measurement that yielded a maximal peak value of 5−10 mV. In contrast, UW-PSII had a very low absolute signal; the maximal peak value of only 1.5−2.5 mV was obtained with 10 $\mu$g of Ch per measurement. In the other samples, where 5 $\mu$g of Chl was used per measurement, the following maximal peak values were observed: 2.4−4 mV for SW-PSII; 1.3−2 mV for PSII reconstituted with WT PsbO; 0.6−0.9 mV for PSII reconstituted with ΔG3M; 0.5−0.9 mV for PSII reconstituted with ΔK14M; and 0.4−0.6 mV for PSII reconstituted with ΔT15M. To compare the $O_2$ yield on the first flash among the samples, all flash yield data were normalized to the height of the peak $O_2$ yield after the third flash, and the results are combined into Figure 3. As can be seen, intact PSII, SW-PSII, and


dx.doi.org/10.1021/bi2008068 |*Biochemistry* 2011, 50, 5988–5998

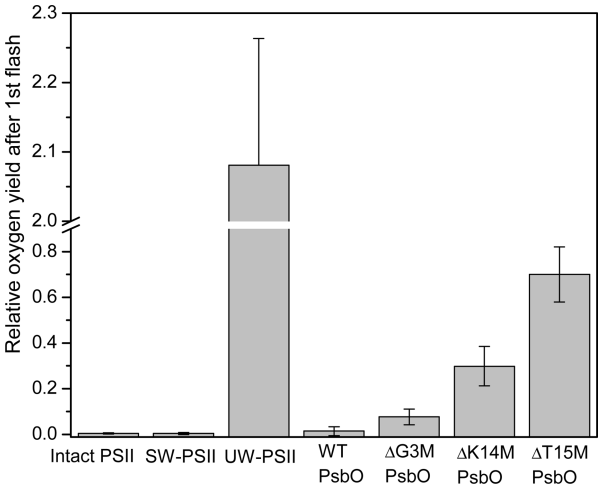


**Figure 3.** Flash $O_2$ yield after the first saturating flash relative to the $O_2$ yield after the third saturating flash. Flashes were applied to intact PSII, SW-PSII, and UW-PSII and to PsbO-depleted PSII reconstituted with WT PsbO, ΔG3M PsbO, ΔK14M PsbO, or ΔT15M PsbO. Data were normalized from the baseline to the height of the third peak ($O_2$ yield after the third saturating flash). Columns are the averages, and vertical bars on each column represent the standard deviation; $n$ = 8−15. Data for WT PsbO and UW-PSII are taken from ref 23 for comparison.

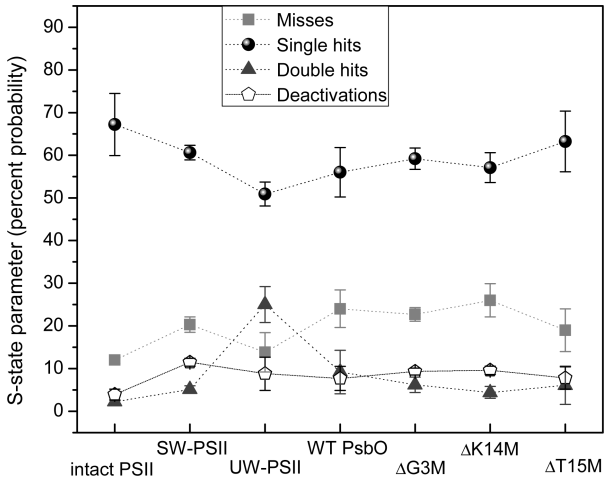


**Figure 4.** S-state parameters for intact PSII, SW-PSII, and UW-PSII and for PsbO-depleted PSII reconstituted with WT PsbO, ΔG3M PsbO, ΔK14M PsbO, or ΔT15M PsbO proteins. Data for WT PsbO and UW-PSII are taken from ref 23 for comparison.

PsbO-depleted PSII reconstituted with WT PsbO (the latter taken from ref 23) exhibit negligible $O_2$ yields on the first flash. For UW-PSII reconstituted with two copies of ΔG3M PsbO, the oxygen yield after the first flash is somewhat higher than that observed for samples containing the native or recombinant WT PsbO protein. Reconstitution of PSII with one copy of ΔK14M PsbO increases the $O_2$ yield on the first flash ∼70-fold relative to the yield observed for intact PSII, while the ΔT15M sample, where one PsbO subunit binds with a low affinity to PSII, exhibits about 170-fold higher $O_2$ yield on the first flash than intact PSII. For comparison, data on PsbO-depleted PSII taken from ref 23 show that this sample has about 500-fold higher $O_2$ yield on the first flash than does intact PSII. These results show that the peak height for $O_2$ yield on the first flash is sensitive to the binding properties of the PsbO deletion mutants and that the amplitude of the $O_2$ yield on the first flash correlates with a decrease in PsbO affinity and stoichiometry in PSII. It is possible that the high $O_2$ yield on the first flash could arise from reactions between electrode-generated $H_2O_2$ and adventitious $Mn^{2+}$ that could be oxidized to $Mn^{3+}$ by a single-turnover flash.[55] This is unlikely to be the case, however. Previous research on PsbO-depleted PSII samples showed that the high $O_2$ yield on the first flash is insensitive to incubation of samples on the electrode with catalase (ref 23, Figure S1, Supporting Information), which eliminates the peroxide-induced signal in PsbO-depleted[56] and PsbP, PsbQ-depleted[57] PSII samples. In addition, other experiments have shown that added peroxide is unable to access intact Mn centers in PSII to produce abnormal $O_2$ flash yields.[57] Finally, the premature flash yield is effectively eliminated by reconstitution of UW-PSII samples with PsbO (Figures 2 and 3). Therefore, the high $O_2$ yield on the first flash in UW-PSII likely arises from a dark-stable population of centers in the $S_2$ or $S_3$ state,[23] where double ($S_2$) or single ($S_3$) hits would produce $O_2$ on the first flash. The decrease in $O_2$ yield on the first flash observed here in PsbO-containing samples (Figures 2 and 3) can be ascribed to an ability of PsbO to decrease the fraction of reaction centers that are arrested in the $S_2$ or $S_3$ states and cannot decay back to $S_1$ in the dark in the absence of PsbO. An increased stability of the higher S-states in the absence of PsbO has been well-documented.[22,25,28,29]

The values of the $O_2$ yields for the first 16 flashes were used to carry out calculations in order to estimate kinetic parameters of S-state turnovers (single and double hits, misses, and deactivation) as well as the S-state distribution of a particular sample at various points during the flash sequence. Figure 4 presents S-state behavior, and Figures 5 and 6 show estimates of the relative amounts of S-states for control and PsbO-reconstituted samples. As can be seen in Figure 4, extraction of the PsbP and PsbQ polypeptides increases somewhat the fractions of misses and deactivations, along with a significant increase in the fraction of double hits for the UW-PSII sample, as compared to all of the other samples, but the parameters are generally equivalent among all of the reconstituted samples (Figure 4). This indicates that binding stoichiometry and affinity of PsbO in reconstituted PSII samples do not have a significant impact on misses, single hits, double hits, or deactivations. As is evident from the data in Figure 4, the major effect of PsbO reconstitution is to repair the defect (the % increase in double hits) caused by its removal. The S-state distributions in Figures 5 and 6 were calculated by fitting data using the four-state homogeneous model that takes into account oxygen production by a single hit to PSII centers in the $S_3$ state but also counts oxygen produced by double hits to centers in the $S_2$ state.[43] An alternative model that takes into account only the centers in the $S_3$ state was also tested with similar results (data not shown). Figures 5 and 6 reveal that at the end of the dark adaptation period (prior to the first flash) the PsbO-depleted sample followed by PSII containing a single weakly bound PsbO subunit (ΔT15M) exhibit smaller populations of centers in the $S_0$ and $S_1$ states and a larger population of centers in $S_3$ as compared to other samples containing native or recombinant PsbO. This indicates that UW-PSII, and to some extent also PSII containing ΔT15M PsbO, contain increased levels of dark-stable $S_2$ and $S_3$ states, in agreement with refs 22 and 23 and with data in Figures 2 and 3. It is also consistent with the observation that a majority of PSII centers after one flash in PsbO-depleted PSII are in the $S_0$ state (Figure 6). Although weak

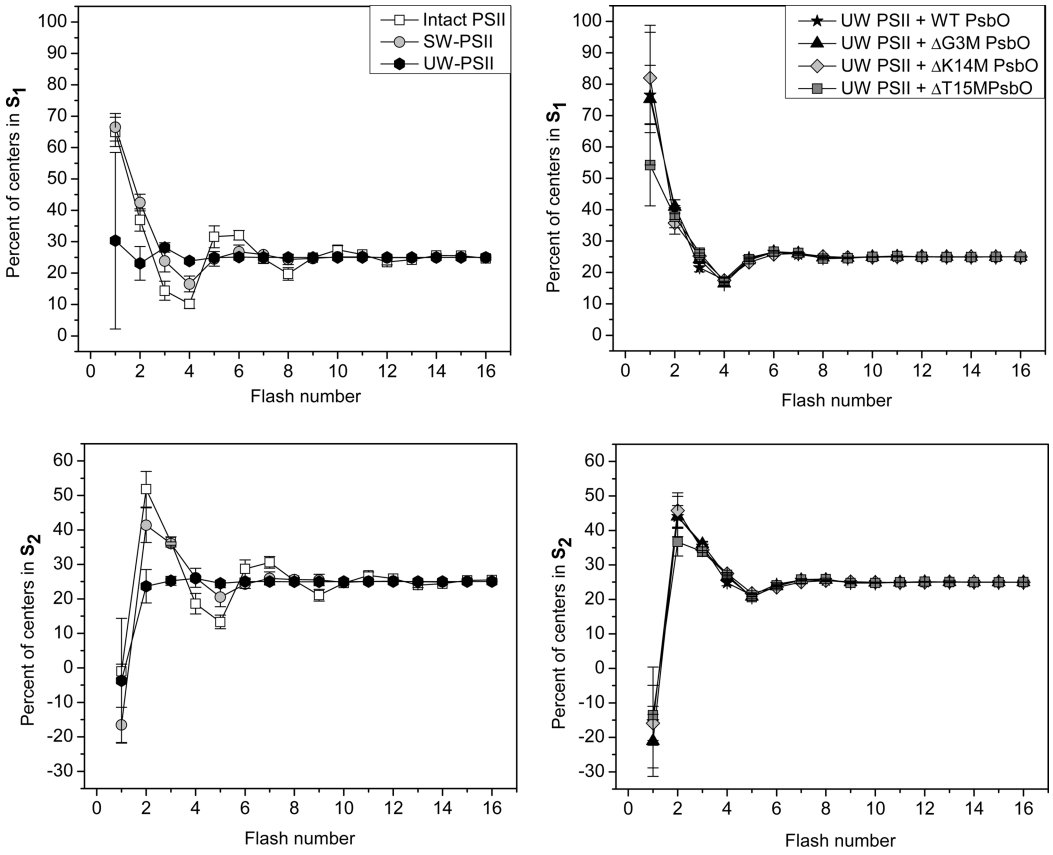


**Figure 5.** Distributions of PSII centers in the $S_1$ and $S_2$ states prior to 1−16 flashes as they were calculated for the controls intact PSII, SW-PSII, and UW-PSII (left panels) and for PsbO-depleted samples reconstituted with WT PsbO, ΔG3M PsbO, ΔK14M PsbO, or ΔT15M PsbO (right panels). Points are the averages, and vertical bars on each point represent the standard deviation; $n$ = 11−12.

rebinding of one PsbO subunit to UW-PSII (ΔT15M) is sufficient, after one flash, to restore an S-state distribution with a majority of PSII centers in the $S_1$ and $S_2$ states, the remaining population of PSII centers in the $S_0$ state is highest of all PsbO-containing samples (Figure 6). This population decreases when one PsbO subunit (ΔK14M) rebinds with a high affinity or when two PsbO subunits are either reconstituted (ΔG3M or WT PsbO) or natively assembled (SW-PSII or intact PSII) into PSII. Taken together, these data suggest that upon binding of the PsbO protein PSII centers display a more typical S-state distribution prior to the second flash, with the majority of centers in the $S_1$ and $S_2$ states and a lower percentage of centers in the $S_0$ state. Differences in these distributions among the deletion mutants correlate with the stoichiometry and binding affinity of the PsbO protein in PSII. With application of further flashes, PsbO binding properties become irrelevant for the S-state distribution, as its patterns prior to 3rd−16th flashes calculated for all PsbO-reconstituted samples are similar to that of SW-PSII (Figures 5 and 6).

To estimate the kinetics of $O_2$-release during the $S_3-[S_4]-S_0$ transition, the rise time of the $O_2$ peaks corresponding to signals after 30−40 flashes were analyzed, by which time the S-states were randomly distributed (Table 4). As the data in Table 4 show, removal of the PsbP and PsbQ polypeptides from PSII does not have a major effect on $O_2$-release kinetics (5 ms for intact PSII vs 9 ms for SW-PSII), as opposed to extraction of PsbO, which extends the $O_2$-release time to 37 ms.[23] Reconstitution of UW-PSII with one PsbO subunit that binds with a low or high affinity shortens the $O_2$-release time to the level (18 ms for ΔT15M and 13 ms for ΔK14M) that is observed for a sample reconstituted with two copies of PsbO (11 ms for WT and 16 ms for ΔG3M), indicating that a single PsbO subunit is sufficient to restore a faster $S_3-[S_4]-S_0$ transition and −O−O− bond formation.

## DISCUSSION

Extraction of PsbO from PSII or its deletion by genetic techniques exacerbates the oxidizing side defects caused by extraction of PsbP and PsbQ; very slow recombination between $Q_A^-$ and the oxidizing side of PSII is observed in samples lacking PsbO[23,24,28] along with greatly decreased steady-state activity coupled with an increased requirement for $Cl^-$ for detection of residual activity and for stability of the $Mn_4Ca$ cluster.[20,58,59] Removal of PsbO also induces a population of long-lived $S_2$ and $S_3$ states in the dark, significantly delays the $O_2$-release time from the OEC, and produces aberrant transitions (especially double hits) relative to samples containing PsbO.[22,23] The results reported here show that PsbO binding stoichiometry, affinity, and specificity affect the extent to which restoration of normal redox reactions on the oxidizing side of PSII can occur.

Although fluorescence curves in Figure 1 show relatively small standard deviations and significant differences among samples, the results in Tables 2 and 3 that fit the decay curves to three phases plus a residual amplitude also generate values for decay times of UW-PSII with large experimental errors that in several


dx.doi.org/10.1021/bi2008068 |*Biochemistry* 2011, 50, 5988–5998

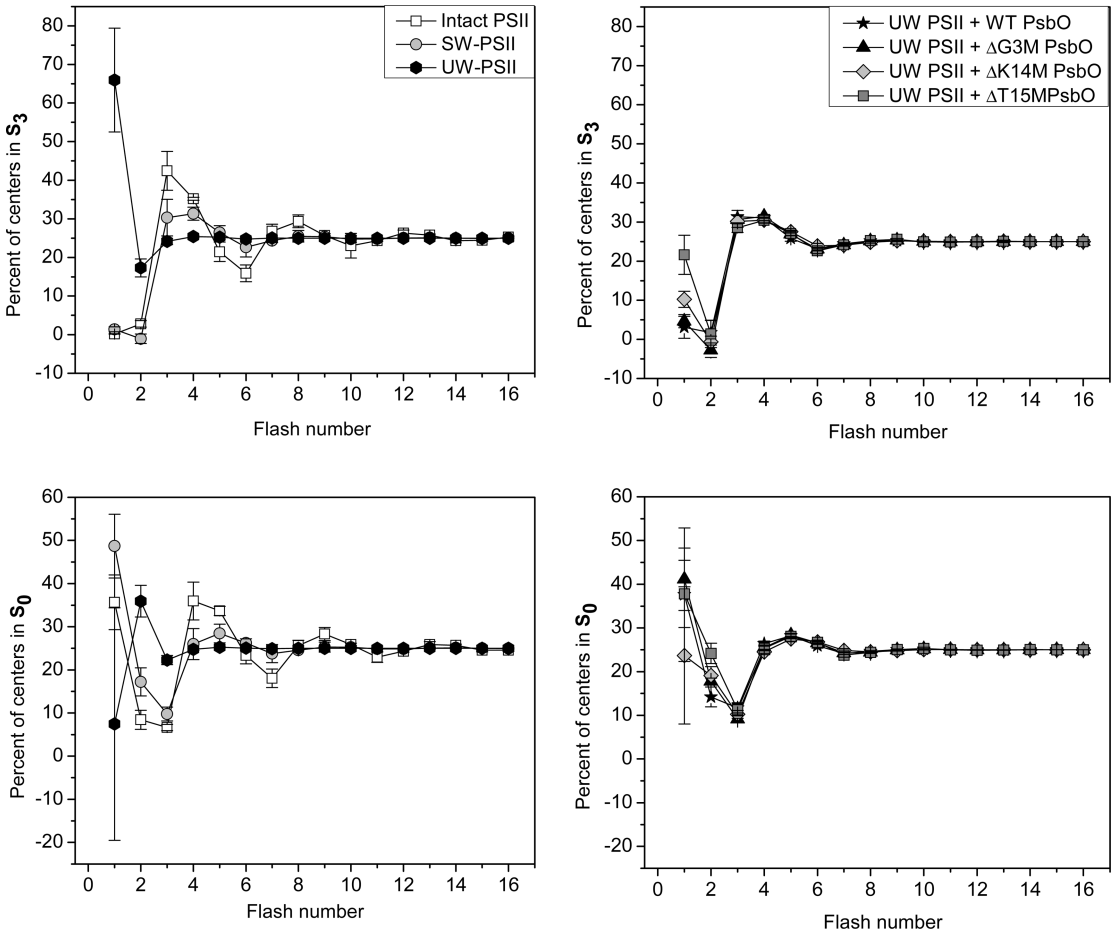


**Figure 6.** Distributions of PSII centers in the $S_3$ and $S_0$ states prior to 1−16 flashes as they were calculated for the controls intact PSII, SW-PSII, and UW-PSII (left panels) and for PsbO-depleted samples reconstituted with WT PsbO, ΔG3M PsbO, ΔK14M PsbO, *or* ΔT15M PsbO (right panels). Points are the averages, and vertical bars on each point represent the standard deviation; $n$ = 11−12.

**Table 4. Oxygen Release Kinetics for Intact PSII, SW-PSII, and UW-PSII Membranes and for PsbO-Depleted PSII Reconstituted with WT PsbO, ΔG3M PsbO, ΔK14M PsbO, or ΔT15M PsbO**

| sample | rise $t_{1/2}$ (ms) | sample | rise $t_{1/2}$ (ms) |
|---|---|---|---|
| intact PSII | 5 ± 1 | UW-PSII + ΔG3M | 16 ± 1 |
| SW-PSII | 9 ± 0 | UW-PSII + ΔK14M | 13 ± 2 |
| UW-PSII | 37 ± 4[b] | UW-PSII + ΔT15M | 18 ± 2 |
| UW-PSII + WT PsbO | 11 ± 1[b] | | |

[b] Data from ref 23 are shown for purposes of comparison ; $n$ = 20−24; error, ±1.0 standard deviation.

cases prevent direct comparisons with the decay times for PsbO-reconstituted samples. The derived amplitudes of the phases are less error-prone, so that in the absence of DCMU (Table 2), the amplitude of the $Q_A^- \rightarrow Q_B$ transition is significantly increased, and the decay time of the slow phase, attributed to a back-reaction between $Q_A^-$ and the oxidizing side, is accelerated in PsbO-reconstituted samples relative to UW-PSII. Results for DCMU-inhibited PSII (Table 3) show that reconstitution with PsbO's increases the amplitudes of the reactions between $Q_A^-$ and $Y_z^\bullet$ (the fast (ms) phase) and between $Q_A^-$ and higher S-states (the intermediate phase) that are likely short-lived.[42] The slow phase is assigned to a similar back-reaction with higher S-states that are in this phase rather stable,[42] and its amplitude is diminished by reconstitution with PsbO's. Taken together, where comparisons with a UW-PSII control are possible, the fluorescence decay data indicate that rebinding of PsbO with increasing stoichiometry and binding affinity has increased the extent of electron transfer on the oxidizing side of PSII and, in the absence of DCMU, increased the rate of recombination between $Q_A^-$ and the OEC.

As can be seen in Figures 2 and 3, UW-PSII samples produce $O_2$ on the first flash. From the absolute signal values for the maximum $O_2$ pulse, given in the Results section, it can be estimated that between 30% and 45% of centers in the UW-PSII sample are responsible for the $O_2$ released on the first flash as compared to centers in a SW-PSII control. While it is possible that some of this signal might originate from peroxide generated by the Pt electrode, prior research,[55−57] our own results (ref 23, Figure S1 of the Supporting Information), and the ability of PsbO reconstitution (Figures 2 and 3) to diminish this $O_2$ peak indicate that peroxide is unlikely to be the major source of $O_2$ in these experiments. The data from Figures 2−6 provide additional insights into the nature of the lesion on the oxidizing side of PSII in UW-PSII and the repair of that lesion by PsbO. An analysis of the defect in UW-PSII (Figure 4) reveals itself in an increase in double hits and a decrease in single turnovers, which indicates, in agreement with data in Figures 5 and 6, that a


dx.doi.org/10.1021/bi2008068 |*Biochemistry* 2011, 50, 5988–5998

UW-PSII sample retains a population of dark-stable $S_3$ and $S_2$ states that produce $O_2$ on a single or a double hit initiated by the first flash. Although weak rebinding of a single copy of PsbO to PSII is sufficient to induce significant changes in the OEC (a near-normal S-state distribution, a $S_3-[S_4]-S_0$ transition and −O−O− bond formation along with a substantially decreased $O_2$ yield on the first flash), these changes, which are evident in samples probed with single turnover flashes, cannot support multiple cycling of the OEC, as documented by low steady-state activity of PSII reconstituted with ΔT15M PsbO.[40] An increase in binding affinity of a single subunit (ΔK14M) of PsbO to PSII is necessary to further restore normal functions on the PSII oxidizing side (Figures 2−6 and Table 4), which contributes to the long-term efficiency and stability of the OEC, as evidenced by the recovery of robust steady state rates of activity.[20,36] Rebinding of a second PsbO subunit to PSII (WT PsbO or ΔG3M PsbO) is necessary to further improve the efficiency of light-driven cycling of the OEC that was established by rebinding of the first PsbO subunit. On the other hand, nonspecific binding of PsbO to PSII has no functional significance in these reactions, which reinforces the conclusions reported in ref 20.

The function of PsbO in PSII was originally thought to involve a direct role, perhaps metal ligation by the protein in assuring stability of the Mn cluster.[60] Had this been true, then removal of PsbO, as in the experiments reported here, might be proposed to modulate the redox potential of the OEC and in that way affect oxidizing side electron transfer. Crystal structures of PSII place PsbO close to, but not in direct contact with, the site of $H_2O$ oxidation, making metal ligation and/or direct effects on redox potentials unlikely.[61,62] So far, there is no evidence to link PsbO to binding of $Ca^{2+}$ in the OEC, but results of a number of experiments point to a role of PsbO in $Cl^-$ retention.[19−21,58,59] UW-PSII shows an increased requirement for $Cl^-$ to support steady-state $O_2$ evolution activity, and various mutations in PsbO, including those used in these experiments,[19−21] have been shown to impair the ability of the protein to support $Cl^-$-dependent $O_2$ evolution activity. Lines of evidence that show an effect of loss of PsbO and/or $Cl^-$ on the stability of higher S-states come from thermoluminescence experiments (induction of stable higher S-states),[25,63,64] from analyses of S-state lifetimes monitored by UV absorbance changes assigned to $Cl^-$ -dependent Mn oxidation state changes,[65,66] and from EPR experiments on the effects of $Cl^-$ depletion on the formation and lifetime of the $S_2$ multiline signal.[67] In the case of EPR experiments, the $S_2$ lifetime after $Cl^-$ depletion was about 10 min vs 10 s for the control,[67] while in the case of thermoluminescence measurements,[64] the $S_2$ $Q_A^-$ lifetime was 92 s after $Cl^-$ depletion as compared to 3 s in the control. A PSII sample depleted of PsbO by the same method used in the present study and assayed in the presence of 20 mM $Cl^-$ produced an $S_2$ $Q_A^-$ lifetime of 36 s,[64] comparable to the slow phase of the control UW-PSII sample in Table 3. Other thermoluminescence experiments[63] and monitoring of the effects of $Cl^-$ on UV absorbance changes[65] have shown that $Cl^-$ loss blocks S-state advancement beyond $S_3$. It is therefore probable that the appearance of populations of stable $S_2$ and $S_3$ states in the UW-PSII samples is due to the consequence of PsbO depletion, namely an inability of these populations of higher S-states states to effectively retain $Cl^-$,[68] coupled with a block in the S-state cycle between $S_3$ and $S_4$. The ability of various mutated PsbO's to restore normal S-state distributions, as presented here, correlates with the efficacies of these proteins in restoring $Cl^-$ retention by the OEC, as revealed in steady-state activity assays.[19−21] These results are consistent with earlier results showing that $Cl^-$ is required to facilitate advancement from $S_2 \rightarrow S_4 \rightarrow S_0$.[65] Why $Cl^-$ removal should stabilize higher S-states is not clear at this time. Crystal structures of PSII are at best models of the $S_1$ (or lower states),[61,62] while the effects of $Cl^-$ on the behavior of the OEC in native PSII reaction centers are only detected after flash formation of higher S-states[65,66] or under steady-state illumination.[67] Any of the proposals for $Cl^-$ function (a Mn ligand in higher S-states, facilitation of $H^+$ transport away from the OEC[69,70]) might be invoked as a potential cause for the stabilization of higher S-states. Experiments to better define the role of pH and $Cl^-$ with respect to the ability of PsbO to restore $O_2$ evolution activity in PSII are now underway.

## ■ ASSOCIATED CONTENT

**Supporting Information.** Figure S1 showing the typical flash $O_2$ yield patterns from UV-PSII in the absence or presence of catalase. This material is available free of charge via the Internet at http://pubs.acs.org.

## ■ AUTHOR INFORMATION

### Corresponding Author

*Tel: (734) 764-9543. Fax: (734) 647-0884. E-mail: popelka@umich.edu.

### Funding Sources

This research was supported by grant to H.P. and C.F.Y. from the National Science Foundation (MCB- 0716541) and by grant to J.L.R. from the USDA National Institute of Food and Agriculture (National Research Initiative Competitive Grant 2008-35318-04605).

## ■ ABBREVIATIONS

BSA, bovine serum albumin; Chl, chlorophyll; DCMU, 3-(3,4-dichlorophenyl)-1,1-dimethylurea; MES, 2-(*N*-morpholino)ethanesulfonic acid; OEC, oxygen-evolving complex; PS, photosystem; PsbO, the manganese-stabilizing protein; $Q_{A(B)}$, primary (secondary) quinone acceptor of PSII; WT PsbO, recombinant wild-type PsbO.

## ■ REFERENCES

(1) Nelson, N., and Yocum, C. F. (2006) Structure and function of photosystems I and II. *Annu. Rev. Plant Biol. 57*, 521–565.

(2) Guskov, A., Gabdulkhakov, A., Broser, M., Glöckner, C., Hellmich, J., Kern, J., Frank, J., Müh, F., Saenger, W., and Zouni, A. (2010) Recent progress in the crystallographic studies of Photosystem II. *ChemPhysChem 11*, 1160–1171.

(3) Debus, R. J. (2008) Protein ligation of the photosynthetic oxygen-evolving center. *Coord. Chem. Rev. 252*, 244–258.

(4) Yocum, C. F. (2008) The calcium and chloride requirements of the $O_2$ evolving complex. *Coord. Chem. Rev. 252*, 296–305.

(5) Kok, B., Forbush, B., and Mcgloin, M. (1970) Cooperation of charges in photosynthetic $O_2$ evolution-I. A linear four step mechanism. *Photochem. Photobiol. 11*, 457–475.

(6) Bricker, T. M., and Burnap, R. L. (2005) The extrinsic proteins of photosystem II, in *Photosystem II: the light-driven water:plastoquinone oxidoreductase* (Wydrzynski, T. J., and Satoh, K., Eds.) Vol. 22, pp 95−120, Springer, Dordrecht, The Netherlands.

(7) De Las Rivas, J., and Roman, A. (2005) Structure and evolution of the extrinsic proteins that stabilize the oxygen-evolving engine. *Photochem. Photobiol. Sci. 4*, 1003–1010.

(8) De Las Rivas, J., Heredia, P., and Roman, A. (2007) Oxygen-evolving extrinsic proteins (PsbO, P, Q, R): Bioinformatics and functional analysis. *Biochim. Biophys. Acta 1767*, 575–582.

(9) Roose, J. L., Wegener, K. M., and Pakrasi, H. B. (2007) The extrinsic proteins of photosystem II. *Photosynth. Res. 92*, 369–387.

(10) Enami, I., Okumura, A., Nagao, R., Suzuki, T., Iwai, M., and Shen, J.-R. (2008) Structures and functions of the extrinsic proteins of photosystem II from different species. *Photosynth. Res. 98*, 349–363.

(11) Ifuku, K., Ishihara, S., Shimamoto, R., Ido, K., and Sato, F. (2008) Structure, function, and evolution of the PsbP protein family in higher plants. *Photosynth. Res. 98*, 427–437.

(12) Thornton, L. E., Ohkawa, H., Roose, J. L., Kashino, Y., Keren, N., and Pakrasi, H. B. (2004) Homologs of plant PsbP and PsbQ proteins are necessary for regulation of photosystem II activity in the cyanobacterium *Synechocystis* 6803. *Plant Cell 16*, 2164–2175.

(13) Miyao, M., and Murata, N. (1984) Calcium ions can be substituted for the 24-kDa polypeptide in photosynthetic oxygen evolution. *FEBS Lett. 168*, 118–120.

(14) Ghanotakis, D. F., Babcock, G. T., and Yocum, C. F. (1984) Calcium reconstitutes high rates of oxygen evolution in polypeptide depleted photosystem II preparations. *FEBS Lett. 167*, 127–130.

(15) Yi, X., Hargett, S. R., Liu, H., Frankel, L. K., and Bricker, T. M. (2007) The PsbP protein is required for Photosystem II complex assembly/stability and photoautotrophy in *Arabidopsis thaliana*. *J. Biol. Chem. 282*, 24833–24841.

(16) Yi, X., Hargett, S. R., Frankel, L. K., and Bricker, T. M. (2006) The PsbQ protein is required in *Arabidopsis* for Photosystem II assembly/stability and photoautotrophy under low light conditions. *J. Biol. Chem. 281*, 26260–26267.

(17) Hutchison, R. S., Steenhuis, J. J., Yocum, C. F., Razeghifard, M. R., and Barry, B. A. (1999) Deprotonation of the 33 kDa, extrinsic, manganese-stabilizing subunit accompanies photooxidation of manganese in Photosystem II. *J. Biol. Chem. 274*, 31987–31995.

(18) Hong, S. K., Pawlikowski, S. A., Vander Meulen, K. A., and Yocum, C. F. (2001) The oxidation state of the Photosystem II manganese cluster influences the structure of manganese stabilizing protein. *Biochim. Biophys. Acta 1504*, 262–274.

(19) Popelkova, H., Betts, S. D., Lydakis-Simantiris, N., Im, M. M., Swenson, E., and Yocum, C. F. (2006) Mutagenesis of basic residues R151 and R161 in manganese-stabilizing protein of photosystem II causes inefficient binding of chloride to the oxygen evolving complex. *Biochemistry 45*, 3107–3115.

(20) Popelkova, H., Commet, A., Kuntzleman, T., and Yocum, C. F. (2008) Inorganic cofactor stabilization and retention: The unique functions of the two PsbO subunits of eukaryotic Photosystem II. *Biochemistry 47*, 12953–12600.

(21) Popelkova, H., Commet, A., and Yocum, C. F. (2009) Asp157 is required for the function of PsbO, the Photosystem II manganese-stabilizing protein. *Biochemistry 48*, 11920–11928.

(22) Miyao, M., Murata, N., Lavorel, J., Maison-Peteri, B., Boussac, A., and Etienne, A.-L. (1987) Effect of the 33-kDa protein on the S-state transitions in photosynthetic oxygen evolution. *Biochim. Biophys. Acta 890*, 151–159.

(23) Roose, J. L., Yocum, C. F., and Popelkova, H. (2010) Function of PsbO, the photosystem II manganese-stabilizing protein: Probing the role of Aspartic Acid 157. *Biochemistry 49*, 6042–6051.

(24) Roose, J. L., Frankel, L. K., and Bricker, T. M. (2010) Documentation of significant electron transport defects on the reducing side of Photosystem II upon removal of the PsbP and PsbQ extrinsic proteins. *Biochemistry 49*, 36–41.

(25) Burnap, R. L., Shen, J.-R., Jursinic, P. A., Inoue, Y., and Sherman, L. A. (1992) Oxygen yield and thermoluminiscence characteristics of a cyanobacterium lacking the manganese-stabilizing protein of photosystem II. *Biochemistry 31*, 7404–7410.

(26) Razeghifard, M. R., Wydrzynski, T., Pace, R. J., and Burnap, R. L. (1997) $Y_z^{\bullet}$ reduction kinetics in the absence of the manganese-stabilizing protein of photosystem II. *Biochemistry 36*, 14474–14478.

(27) Murakami, R., Ifuku, K., Takabayashi, A., Shikanai, T., Endo, T., and Sato, F. (2002) Characterization of an *Arabidopsis thaliana* mutant with impaired psbO, one of two genes encoding extrinsic 33-kDa proteins in photosystem II. *FEBS Lett. 523*, 138–142.

(28) Liu, H., Frankel, L. K., and Bricker, T. M. (2007) Functional analysis of photosystem II in a PsbO-1-deficient mutant in *Arabidopsis thaliana*. *Biochemistry 46*, 7607–7613.

(29) Bricker, T. M., and Frankel, L. K. (2008) The *psbo1* mutant of *Arabidopsis* cannot efficiently use calcium in support of oxygen evolution by photosystem II. *J. Biol. Chem. 283*, 29022–290−27.

(30) Yi, X., McChargue, M., Laborde, S., Frankel, L. K., and Bricker, T. M. (2005) The manganese-stabilizing protein is required for photosystem II assembly/stability and photoautotrophy in higher plants. *J. Biol. Chem. 280*, 16170–16174.

(31) Mayfield, S. P., Bennoun, P., and Rochaix, J. D. (1987) Expression of the nuclear encoded OEE1 protein is required for oxygen evolution and stability of photosystem II particles in *Chlamydomonas reinhardtii*. *EMBO J. 6*, 313–318.

(32) Xu, Q., and Bricker, T. M. (1992) Structural organization of proteins on the oxidizing side of photosystem II: 2 Molecules of the 33-kDa manganese-stabilizing proteins per reaction center. *J. Biol. Chem. 267*, 25816–25821.

(33) Seidler, A. (1994) Introduction of a histidine tail at the N-terminus of a secretory protein expressed in *Escherichia coli*. *Protein Eng. 7*, 1277–1280.

(34) Leuschner, C., and Bricker, T. M. (1996) Interaction of the 33 kDa extrinsic protein with photosystem II: Rebinding of the 33 kDa extrinsic protein to photosystem II membranes which contain four, two, or zero manganese per photosystem II reaction center. *Biochemistry 35*, 4551–4557.

(35) Betts, S. D., Ross, J. R., Pichersky, E., and Yocum, C. F. (1997) Mutation Val235Ala weakens binding of the 33-kDa manganese stabilizing protein of photosystem II to one of two sites. *Biochemistry 36*, 4047–4053.

(36) Popelkova, H., Im, M. M., and Yocum, C. F. (2002) N-terminal truncations of manganese stabilizing protein identify two amino acid sequences required for binding of the eukaryotic protein to photosystem II and reveal the absence of one binding-related sequence in cyanobacteria. *Biochemistry 41*, 10038–10045.

(37) Murakami, R., Ifuku, K., Takabayashi, A., Shikanai, T., Endo, T., and Sato, F. (2005) Functional dissection of two *Arabidopsis* PsbO proteins. *FEBS J. 272*, 2165–2175.

(38) Popelkova, H., and Yocum, C. F. (2011) PsbO, the manganese-stabilizing protein: Analysis of the structure-function relations that provide insights into its role in Photosystem II. *J. Photochem. Photobiol., B*in press.

(39) Popelkova, H., Im, M. M., D'Auria, J., Betts, S. D., Lydakis-Simantiris, N., and Yocum, C. F. (2002) N-terminus of the photosystem II manganese stabilizing protein: Effects of sequence elongation and truncation. *Biochemistry 41*, 2702–2711.

(40) Popelkova, H., Im, M. M., and Yocum, C. F. (2003) Binding of manganese stabilizing protein to photosystem II: Identification of essential N-terminal threonine residues and domains that prevent nonspecific binding. *Biochemistry 42*, 6193–6200.

(41) Nedbal, L., Trtilek, M., and Kaftan, D. (1999) Flash fluorescence induction: a novel method to study regulation of Photosystem II. *J. Photochem. Photobiol. 48*, 154–157.

(42) Reifarth, F., Christen, G., Seeliger, A. G., Dorman, P., Benning, C., and Renger, G. (1997) Modification of the water oxidizing complex in leaves of the *dgd1* mutant of *Arabidopsis thaliana* deficient in the galactolipid digalactosyldiacylglycerol. *Biochemistry 36*, 11769–11776.

(43) Meunier, P. C. (1993) Oxygen evolution by Photosystem II − The contributions of backward transitions to the anomalous behavior of double-hits revealed by a new analysis method. *Photosynth. Res. 36*, 111–118.

(44) Bowes, J., and Crofts, A. R. (1980) Binary oscillations in the rate of reoxidation of the primary acceptor of photosystem II. *Biochim. Biophys. Acta 590*, 373–389.

(45) Weiss, W., and Renger, G. (1984) Analysis of the system II reaction by UV-absorption changes in Tris-washed chloroplasts, in *Advances in Photosynthesis Research* (Sybesma, C., Ed.) pp 167−170, Martinus Nijhoff, The Hague, The Netherlands.

(46) Renger, G., Gleiter, H. M., Haag, E., and Reifarth, F. (1993) Photosystem II: Thermodynamics and kinetics of electron transport from $Q_A^-$ to $Q_B$ and to $Q_B^-$ and deleterious effects of copper. *Z. Naturforsch. 48c*, 234–250.

(47) Crofts, A. R., and Wraight, C. A. (1983) The electrochemical domain of photosynthesis. *Biochim. Biophys. Acta 726*, 149–186.

(48) Robinson, H. H., and Crofts, A. R. (1983) Kinetics of the oxidation reduction reactions of the photosystem II quinone acceptor complex and the pathway for deactivation. *FEBS Lett. 153*, 221–226.

(49) Weiss, W., and Renger, G. (1984) UV spectral characterization in Tris-washed chloroplasts of the redox component-D1 which functionally connects the reaction center with the water-oxidizing enzyme system-Y in photosynthesis. *FEBS Lett. 169*, 219–223.

(50) Ghanotakis, D. F., Babcock, G. T., and Yocum, C. F. (1984) Calcium reconstitutes high rates of oxygen evolution in polypeptide depleted photosystem II preparations. *FEBS Lett. 167*, 127–130.

(51) Ghanotakis, D. F., O'Malley, P. J., Babcock, G. T., and Yocum, C. F. (1983) Structure and inhibition of components on the oxidizing side of photosystem II, in *The Oxygen Evolving System of Photosynthesis* (Inoue, Y., Crofts, A. R., Govindjee, M. N., Renger, G., and Satoh, K., Eds.) pp 91−101, Academic Press, Tokyo, Japan.

(52) Chroni, S., and Ghanotakis, D. F. (2001) Accessibility of tyrosine $Y_Z^{\bullet}$ to exogenous reductants and $Mn^{2+}$ in various photosystem II preparations. *Biochim. Biophys. Acta 1504*, 432–437.

(53) Debus, R. J. (1992) The manganese and calcium ions of photosynthetic oxygen evolution. *Biochim. Biophys. Acta 1102*, 269–352.

(54) Seibert, M., and Lavorel, J. (1983) Oxygen-evolution patterns from spinach photosystem II preparations. *Biochim. Biophys. Acta 723*, 160–168.

(55) Mano, J., Takahashi, M., and Asada, K. (1987) Oxygen evolution from hydrogen peroxide in photosystem II: Flash-induced catalytic activity of water-oxidizing photosystem II membranes. *Biochemistry 26*, 2495–2501.

(56) Berg, S. P., and Seibert, M. (1987) Is functional manganese involved in hydrogen-peroxide-stimulated anomalous oxygen evolution in $CaCl_2$-washed photosystem II membranes?. *Photosynth. Res. 13*, 3–17.

(57) Schroder, W. P., and Akerlund, H.-E. (1986) $H_2O_2$ accessibility to the photosystem II donor side in protein-depleted inside-out thylakoids measured as flash-induced oxygen production. *Biochim. Biophys. Acta 848*, 359–363.

(58) Miyao, M., and Murata, M. (1984) Role of the 33-kDa polypeptide in preserving Mn in the photosynthetic oxygen-evolution system and its replacement by chloride ions. *FEBS Lett. 170*, 350–354.

(59) Bricker, T. M. (1992) Oxygen evolution in the absence of the 33 kDa manganese-stabilizing protein. *Biochemistry 31*, 4623–4628.

(60) Kuwabara, T., and Murata, N. (1983) Analysis of the inactivation of photosynthetic oxygen evolution and the release of polypeptides and manganese in the photosystem II particle of spinach chloroplasts. *Plant Cell Physiol. 24*, 741–747.

(61) Guskov, A., Kern, J., Gabdulkhakov, A., Broser, M., Zouni, A., and Saenger, W. (2009) Cyanobacterial photosystem II at 2.9 Å resolution and the role of quinones, lipids, channels, and chloride. *Nat. Struct. Mol. Biol. 16*, 334–342.

(62) Umena, Y., Kawakami, K., Shen, J.-R., and Kamiya, N. (2011) Crystal structure of oxygen-evolving photosytem II at a resolution of 1.9 Å. *Nature 473*, 55–60.

(63) Homann, P. H., Gleiter, H., Ono, T.-a., and Inoue, Y. (1986) Storage of abnormal oxidants '$\Sigma_1$', '$\Sigma_2$', and '$\Sigma_3$' in photosynthetic water oxidases inhibited by $Cl^-$-removal. *Biochim. Biophys. Acta 850*, 10–20.

(64) Vass, I., Ono, T.-A., and Inoue, Y. (1987) Stability and oscillation properties of thermoluminescent charge pairs in the $O_2$-evolving system depleted of $Cl^-$ or the 33 kDa extrinsic protein. *Biochim. Biophys. Acta 892*, 224–235.

(65) Wincencjusz, H., van Gorkom, H. J., and Yocum, C. F. (1997) The photosynthetic oxygen evolving complex requires chloride for its redox state $S_2 \rightarrow S_3$ and $S_3 \rightarrow S_0$ transitions but not for $S_0 \rightarrow S_1$ or $S_1 \rightarrow S_2$ transitions. *Biochemistry 36*, 3663–3670.

(66) Wincencjusz, H., Yocum, C. F., and van Gorkom, H. J. (1999) Activating anions that replace $Cl^-$ in the $O_2$ evolving complex of photosystem II slow the kinetics of the terminal step in water oxidation and destabilize the $S_2$ and $S_3$ states. *Biochemistry 38*, 3719–3725.

(67) Ono, T., Zimmermann, J. L., Inoue, Y., and Rutherford, A. W. (1985) EPR evidence for a modified S-state transition in chloride-depleted photosystem II. *Biochim. Biophys. Acta 851*, 193–201.

(68) Wincencjusz, H., Yocum, C. F., and van Gorkom, H. J. (1998) S-state dependence of chloride binding affinities and exchange dynamics in the intact and polypeptide-depleted $O_2$-evolving complex of photosystem II. *Biochemistry 37*, 8595–8604.

(69) Popelkova, H., and Yocum, C. F. (2007) Current status of the role of $Cl^-$ ion in the oxygen-evolving complex. *Photosynth. Res. 93*, 111–121.

(70) Pokhrel, R., McConnell, I. L., and Brudvig, G. W. (2011) Chloride regulation of enzyme turnover: Application to the role of choride in photosystem II. *Biochemistry 50*, 2725–2734.